Advances in Science and Technology Research Journal

Advances in Science and Technology Research Journal, 2026, 20(8), 252–268
https://doi.org/10.12913/22998624/220821
ISSN 2299-8624, License CC-BY 4.0

Received: 2026.03.09
Accepted: 2026.06.01
Published: 2026.07.01

The concept of recovering electrical energy in a car trailer

Dariusz Więckowski[1*], Karol Bocheński[2], Tomasz Pusty[3]

[1] Faculty of Automotive and Construction Machinery Engineering, Warsaw University of Technology, ul. Narbutta 84, 02-524 Warsaw, Poland
[2] Quasar Electronics, ul. 25K Cieślewskich, 03-017 Warsaw, Poland
[3] Department of Machine Construction, Maritime University of Szczecin, ul. Willowa 2, 71-650 Szczecin, Poland
* Corresponding author's e-mail: dariusz.wieckowski@pw.edu.pl

ABSTRACT

This paper addresses the implementation of an energy recovery system in a category O2 trailer. Energy recovery systems for transport, including regenerative braking in hybrid (HEV) and battery-electric (BEV) vehicles, are reviewed. Two main regenerative braking strategies are presented and discussed: serial and parallel. Solutions for braking systems in O1 and O2 trailers are discussed, focusing on the two most popular solutions: electric and overrun. The overrun system was chosen as the basis for further work due to its simple design and popularity in trailer applications. The next section of the paper presents the concept of an electric energy recovery system in a trailer. A modification of the driving axle of a fully refrigerated trailer is proposed. The system utilizes an electric motor operating solely in generator mode. Concepts for controlling the electromagnetic clutch are developed based on signals from the IVECO DAILY vehicle's CAN bus. Traction calculations were performed for an IVECO eDaily electric vehicle in four variants: without a trailer, with an empty trailer, with half the permissible trailer load, and with a full trailer load. The results indicated a significant effect of the trailer weight on the traction characteristics of the vehicle and trailer combination. A key element of the work was the development of a simulation model in MatLab Simulink, which performs calculations based on the relevant relationships specified in the work. Simulation studies were conducted for four driving profiles: a standardized WLTC cycle and three actual cycles recorded by the author. Each cycle was tested with three trailer load variants. The highest value of recovered energy was 5.4 kWh, which would allow a 1.6 kW refrigeration unit to operate for 3.5 hours, bringing economic and environmental benefits. Based on the simulation studies and the entire workflow, the obtained results were summarized, conclusions were drawn, and further research was proposed.

Keywords: car trailer, regenerative braking, energy recovery, CAN bus.

INTRODUCTION

In an era of increasing electrification, hybrid and electric vehicles are gaining a growing presence on the roads. According to a report by The European Automobile Manufacturers' Association ACEA, in the first eight months of 2025, the share of newly registered fully electric cars (BEV – battery electric vehicle) in the European Union was 15.8%, and hybrid vehicles (HEV – hybrid electric vehicle) 43.5% [1]. The braking system of a traditional combustion engine vehicle dissipates the vehicle's kinetic energy during braking, converting it into heat. This energy conversion means irreversible loss. In electric and hybrid systems, some of the vehicle's kinetic energy can be recovered. In drives using electric machines, the ability of the electric motor to operate in reverse (generator mode) is utilized. Generator mode is used during braking or downhill driving. The electric machine converts the vehicle's kinetic energy into electrical energy and stores the recovered energy as electricity in the batteries. BEV and HEV braking systems are configured so that when the accelerator pedal is released, some energy is recovered by the electric motor, simulating engine braking. Energy recovery occurs

up to a certain vehicle speed limit. Beyond this limit, the electric motor's electromotive force is too low, requiring cooperation with a conventional braking system to bring the vehicle to a complete stop [2]. Energy can be stored in supercapacitors, batteries, energy inertia reels, or fed directly into the traction network [3–5]. The regenerative braking process in HEV and BEV vehicles is managed by a controller that uses information obtained from sensors such as the accelerator and brake pedal angle, steering angle, and vehicle speed. This information is continuously interpreted by the controller and, in the event of an emergency braking, it bypasses the energy recovery system by fully utilizing the friction brakes. The braking controller also distributes braking force between the front and rear axles of the vehicle to effectively reduce speed and maintain a stable driving path. Taking into account information from the vehicle sensors and the above-mentioned requirements, the controller manages the system to recover as much energy as possible [6]. For this purpose, the control algorithm is based on two regenerative braking strategies: serial and parallel [7, 8], Figure 1.

In the series braking strategy, the braking torque generated by the electric motor is used first. The conventional braking system is activated when the braking torque demand exceeds the electric motor's capability. This strategy enables significant kinetic energy recovery. The disadvantage of this solution is the high complexity of the control system. Precise control of the transition between regenerative and friction braking is necessary. An electronic control system for both the electronic and mechanical components of the braking system is required. In the parallel braking strategy, the braking torque is generated simultaneously by the regenerative braking system and the conventional braking system. Using the parallel strategy, the vehicle is unable to recover as much kinetic energy as using the series strategy. The advantage of this algorithm is its simpler design, as there is no need for electronic control of the mechanical component of the braking system [7, 8]. A contemporary innovative application of regenerative braking is the installation of a modified axle on a tractor-trailer. An example is the AxlePower system, which is designed to power refrigerated truck semitrailers – Figure 2 [9]. The AxlePower system utilizes energy recovered during braking and then stores it in an energy storage unit located in the semitrailer chassis. A fully charged battery pack allows for two hours of autonomous operation of the refrigerated truck. The entire system is mounted in the trailer, making it completely independent of the type of tractor unit. Additionally, the modified semitrailer is equipped with an intelligent power management system that allows for independent switching between three operating modes, ensuring the highest efficiency of recovered energy. The system features the following operating modes: regenerative braking, active, and active with fast charging. Regenerative mode recovers energy during braking of the tractor unit and semitrailer. Active mode charges the trailer battery while driving on flat terrain when the system detects a power shortage. Fast charging mode is designed for driving cycles with an inefficient distance-to-idle time ratio, ensuring a fully charged battery for extended operation at each stop [9].

Although the concept of energy recovery is well established in HEV and BEV vehicles, its application to light trailers has not been sufficiently explored. This work adapts this concept to an O2 category trailer equipped with a mechanical overrun braking system, including the development of an axle-integrated energy recovery system and a control strategy based on CAN bus signals from the towing vehicle. A simulation model was also developed to analyze the influence of

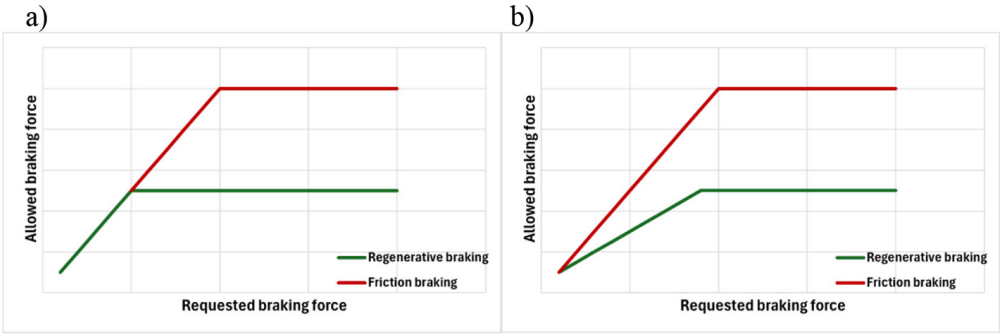

Figure 1. Braking strategy: (a) serial, (b) parallel

Figure 2. AxlePower system [9]

trailer mass and driving profile on the recovered energy. Therefore, the study extends an existing concept into a new technical domain and addresses a research gap related to light trailers.

The concept of recovering electrical energy in a car trailer is increasingly explored as a means of improving energy efficiency and reducing emissions in transport systems. In [40], a trailer axle equipped with a braking energy recovery system using a synchronous reluctance generator and a Matlab Simulink model is presented, demonstrating the feasibility of generating electrical energy to power auxiliary systems such as refrigeration units. This approach aligns with regulatory and system-level analyses described in [41], where the VECTO Trailer methodology highlights the growing importance of electrified trailers and shows that integrating energy recovery systems can significantly reduce CO_2 emissions.

A critical aspect of implementing such systems is the control of regenerative braking. In [42], a dynamic model of a tractor–semitrailer system is used to optimize braking force distribution while maintaining stability, particularly by addressing jackknife risk. Similarly, [43] demonstrates that properly designed braking force distribution strategies based on ECE regulations and fuzzy control can improve energy recovery while preserving braking stability and extending vehicle range.

The effectiveness of energy recovery in trailers is strongly influenced by operating conditions, especially vehicle and trailer mass. In [44], a method for estimating vehicle mass based on dynamic response is proposed, which is essential for accurate modeling and control of energy recovery systems under varying load conditions. Furthermore, safety considerations are crucial when integrating such systems, as shown in [45], where delayed trailer response during emergency maneuvers is identified, and in [46], where appropriate control system parameter selection is necessary to ensure stable obstacle avoidance.

Additional operational factors, such as tire pressure and vehicle configuration analyzed in [47], influence system dynamics and overall performance, while advanced energy management strategies such as the robust approach proposed in [48] demonstrate how adaptive control can optimize energy usage under varying driving conditions. Together, these studies provide a comprehensive foundation for the development of electrical energy recovery systems in car trailers, supporting both technical feasibility and practical implementation.

CAR TRAILER MODEL

In this work, a category O2 trailer was adopted as the research object, which is characterized by the requirement to be equipped with an overrun brake, in accordance with legal regulations for vehicles with a permissible total weight above 750 kg [10]. The calculations and the simulation model were based on the trailer shown in Figure 3. This is a trailer with a total load capacity of 1300 kg.

In the analysed project, it was assumed that the trailer was equipped with a full refrigeration unit, enabling the transport of goods within a controlled temperature range of 3 to 10 °C. This type of refrigeration unit utilizes refrigeration units with a typical power output of 1 to 2 kW. Figure 4 shows the appearance of the unit under consideration.

To implement the energy recovery system, a three-phase 8.5 kW electric motor from the Hyundai Sonata hybrid model [11] was selected, along with a single-speed mechanical transmission, an electromagnetic clutch controlled by a

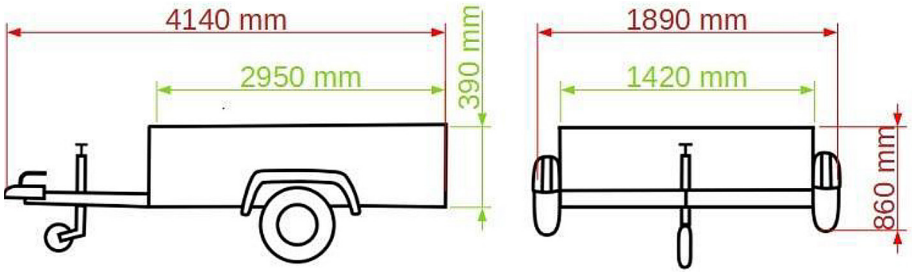

Figure 3. Dimensions of the adopted car trailer

Figure 4. Refrigerated body of a car trailer

signal from the towing vehicle's CAN bus, and an inverter. A schematic of the system is shown in Figure 5.

Model of electric motor with inverter was based on real efficiency map, data required to build efficiency map was obtained from laboratory testing made by Oak Ridge Laboratory [11]. The electric motor used in the project is an 8.5 kW motor from the 2011 Hyundai Sonata Hybrid. The model of electric motor with inverter is shown on Figure 6. Parameters of the selected electric motor: Nominal power 8.5 kW, Instantaneous power 20 kW, Torque 110 Nm, Maximum speed 15,700 rpm, Maximum efficiency 88% [11]. The model determines the instantaneous efficiency values using the rotational speed and torque calculated in the transmission model. The efficiency map is shown on Figure 7. Obtained instantaneous efficiency value was then used to calculated the power. The power is calculated using the formula:

$$P_{sil} = T_{sil} \cdot \omega_{sil} \cdot \eta_{sil} \tag{1}$$

where: P_{sil} – engine power [kW], T_{sil} – engine torque [Nm], ω_{sil} – engine rotational speed [rpm], η_{sil} – engine efficiency [-].

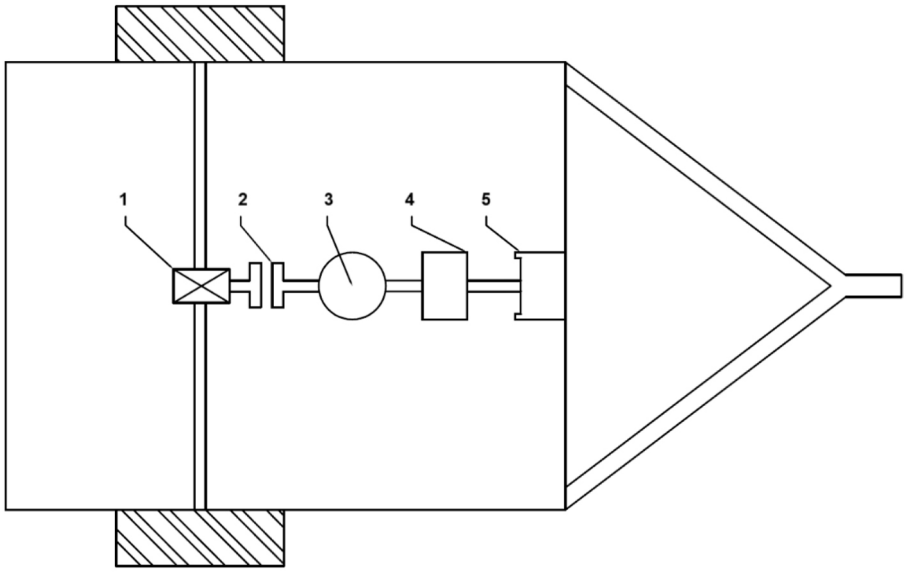

Figure 5. Schematic diagram of a trailer's energy recovery system: 1 – gearbox, 2 – electromagnetic clutch, 3 – electric machine in generator mode, 4 – inverter, 5 – battery

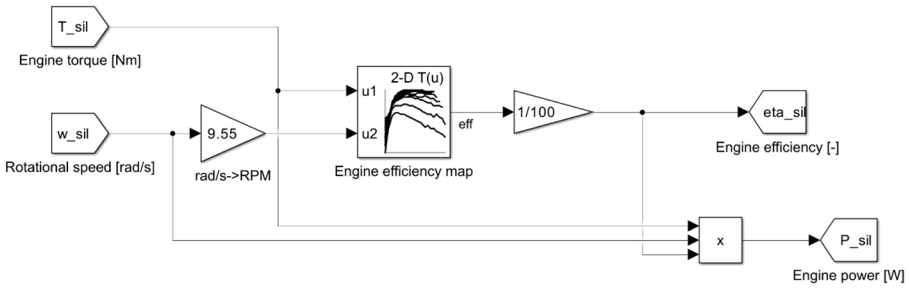

Figure 6. Model of electric model with inverter

In the proposed system, the electric motor is not permanently connected to the trailer axle. Braking torque is transferred by engaging an electromagnetic clutch. The clutch engagement control method adopted for the tested project involves receiving appropriate signals from the towing vehicle's CAN bus. For this purpose, the transmission from the CAN bus of an IVECO Daily vehicle from the 2024 model year was read. Figure 8 shows the location where the IVECO Daily's CAN H and CAN L wires are connected

Clutch activation is designed for several situations: releasing the accelerator pedal, pressing the brake pedal. The detected brake pedal position allows the inverter to control the load on the electric motor. To prevent abrupt clutch engagement, which could quickly damage the clutch, the control system is equipped with a soft-start system. Additionally, readings of engine speed (in the case of the combustion version of the IVECO vehicle) or the 12V battery charge status (in the case of the IVECO eDaily) will activate the charging circuit for the small battery powering the clutch control system. The charging circuit can be implemented using pins 10 and 11 of the 13-pin socket, in compliance with the ISO 11446 standard defining trailer socket wiring [12]. The PCAN-USB-FD

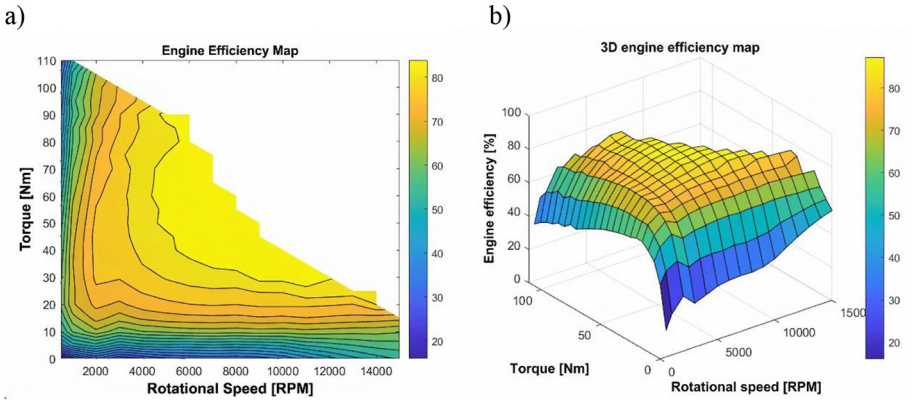

Figure 7. Efficiency maps of 8.5 kW electric motor used in the project: (a) 2D contour plot, (b) 3D surface plot [11]

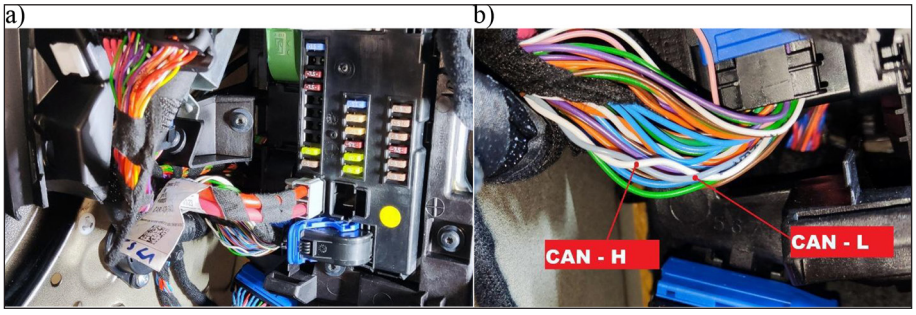

Figure 8. Wiring harness – CAN twisted pair: (a) Fuse socket with wiring harnesses, (b) wiring harness with CAN twisted pair wires specified

interface from PEAK System was used to read data from the IVECO Daily's CAN bus [13].

The transmission was then recorded. PCAN-Explorer 6 software was used to correctly interpret the relevant addresses. The addresses of individual signals in the Iveco CAN bus are compliant with the international J1939 standard [14]. It is based on the CAN bus with 29-bit identifiers and standardizes the way vehicle controllers communicate with each other. Each CAN message in the J1939 standard contains a frame with a specific Parameter Group Number (PGN), which contains several Suspect Parameter Numbers (SPNs). PGN is an 18-bit identification number, typically written in hexadecimal and decimal notation. It defines a group of parameters of a given type sent in a single message. SPN is a unique identifier describing a single parameter; one PGN includes several SPNs [15].

TRACTION CALCULATIONS

The assumed vehicle towing the modified trailer is an IVECO eDaily with a fully electric drive. The vehicle's technical parameters are presented in Table 1 [16, 17].

The rotating (or reduced) mass factor is a dimensionless parameter (always greater than 1) that takes into account the influence of the kinetic energy of rotating vehicle components on the dynamics of motion in calculations. It was determined according to the relationship [18–20]:

$$\delta = 1 + \frac{I_S \cdot i_g^2 \cdot \eta}{m \cdot r_d^2} \cdot i_b^2 + \frac{k \cdot I_k}{m \cdot r_d^2} \tag{2}$$

$$r_d = \lambda \cdot (H + r) \tag{3}$$

where: λ – tire deformation coefficient equal to 0.97 [-]; H – tire height [mm]; r – tire radius [mm].

Table 1. IVECO Daily vehicle parameters [16, 17]

Parameter	Symbol	Value	Unit
Total gear ratio	i_c	13	-
Frontal area	A	5.45	m²
Air drag coefficient	c_x	0.38	-
Current weight	m	2850	kg
Maximum power	P_{iveco}	188	KM
Engine speed at maximum power	-	3750	rpm
Maximum torque	T_{iveco}	400	Nm
Engine speed at maximum torque	-	3750	rpm
Dynamic radius	r_d	0.345	m
Engine moment of inertia	I_s	0.08	kg·m²
Wheel moment of inertia	I_k	1.53	kg·m²
Efficiency	η	0.97	-
Rotating mass coefficient	δ	1.03	-
Final gear ratio	i_g	3.5	-
Gear ratio	i_b	3.6	-

During motion, a moving vehicle is subjected to resistance forces that counteract its movement: rolling resistance, air resistance, inertia resistance, and trailer towing resistance. The design ignores the influence of steering and hill resistance. The effect of road gradient was intentionally neglected as a simplifying assumption in the simulation model. The primary objective of the study was to perform a comparative analysis of the influence of trailer load and driving profile on the amount of recovered energy under consistent and repeatable boundary conditions. Therefore, the model was limited to a flat-road assumption, including the main resistance components, namely rolling resistance, aerodynamic drag, and inertial resistance. Including the road gradient would require the introduction of an additional gravitational force component dependent on the actual elevation profile of a given route, which would significantly reduce the comparability of the analyzed cases. For this reason, the WLTC-based simulations were treated as reference scenarios. However, it should be noted that for routes located in mountainous regions, such as Bielsko-Biała – Liptovský Mikuláš and Ivachnová – Tarnów, neglecting the road gradient may affect the quantitative accuracy of the results. On uphill sections, the energy recovery potential would be lower due to increased tractive effort demand, whereas on downhill sections it could be higher due to the contribution of gravitational forces. Therefore, the presented results should be interpreted as reference values rather than exact route-specific predictions. The inclusion of the road elevation profile is considered a direction for future work. The force system acting on a car trailer is shown in Figure 9 [21, 22].

Balance of trailer forces:

$$\sum F_x = -F_t - F_h + F_b - F_p = 0 \tag{4}$$

$$\sum F_y = R - Q = 0 \tag{5}$$

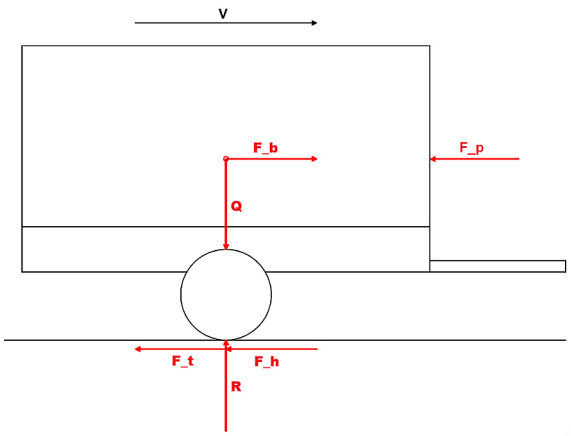

Figure 9. The system of forces acting on the trailer during braking: Q – trailer weight, Fb – inertial resistance force, Fh – braking force, Ft – rolling resistance force, Fp – air resistance force, R – normal reactions [21, 22]

The torque and engine power curves for the IVECO eDaily vehicle are shown in Figure 10a. The graphs were developed based on [16, 17]. The power available at the vehicle's wheels plays an important role when considering vehicle motion. This power is lower than the engine's power due to mechanical losses. The speed-dependent power curve for an IVECO vehicle is shown in Figure 10b.

Wheel power:

$$P_k = P_s \cdot \eta \tag{6}$$

where: P_k – power on the wheels [kW]; P_s – engine power [kW].

The power balance can be used to determine the vehicle's maximum speed. It is located at the intersection of the wheel power curve and the drag force curve. For the vehicle in question, the manufacturer limits the maximum speed to 120 km/h.

Dynamic characteristics – an indicator that allows for easy comparison of vehicle performance characteristics. The dynamic indicator is calculated using the formula [19, 20]:

$$D = \frac{F_n - F_{op}}{m_c \cdot g} \tag{7}$$

where: D – dynamic indicator [-]; F_n – driving force [N]; F_{op} – force of resistance to motion [N]; m_c – total weight of the set [kg].

The driving force of the vehicle was calculated according to the relationship [28, 29]:

$$F_n = \frac{T_s \cdot i_c \cdot \eta}{r_d} \tag{8}$$

where: T_s – engine torque [Nm].

Figure 11 shows the dynamic indicator curves for: the vehicle itself without a trailer, an empty trailer, a trailer with half the maximum trailer load and a trailer with the maximum loa. With increasing speed, the dynamic index value decreases for each tested variant. This is related to increasing motion resistance. The highest dynamic index value is achieved by the vehicle alone without a trailer, which is predictable due to the lower weight of the entire combination. With increasing trailer weight, the index decreases. A heavier load increases both the weight and the motion resistance values. The lowest dynamic index value is achieved by the combination with a fully loaded trailer; this parameter is almost 30% lower. A fully loaded trailer contributes to a significant deterioration in the traction capabilities of the entire system. In this variant, negotiating slopes or overtaking is significantly more difficult. For each variant, the graph ends at a speed of 120 km/h, which is related to the manufacturer's upper limit on the maximum speed. The curves shown above show how closely the dynamic index value is related to the weight of the vehicle + trailer combination. Figure 12 presents the IVECO acceleration curves for all tested variants.

Figure 13a shows the speed characteristics of the standardized WLTC cycle [23]. The average

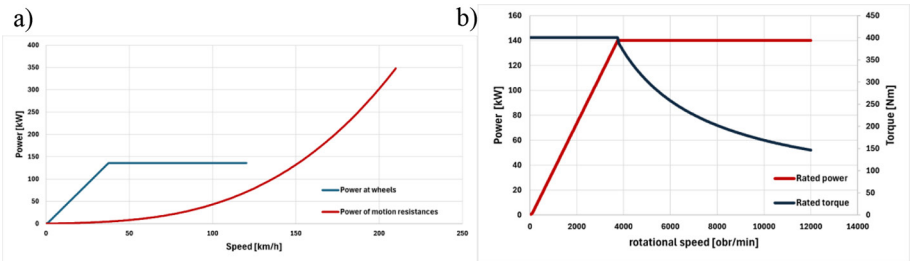

Figure 10. 140 kW engine from IVECO eDaily [16, 17]: a) torque and power graph b) power balance

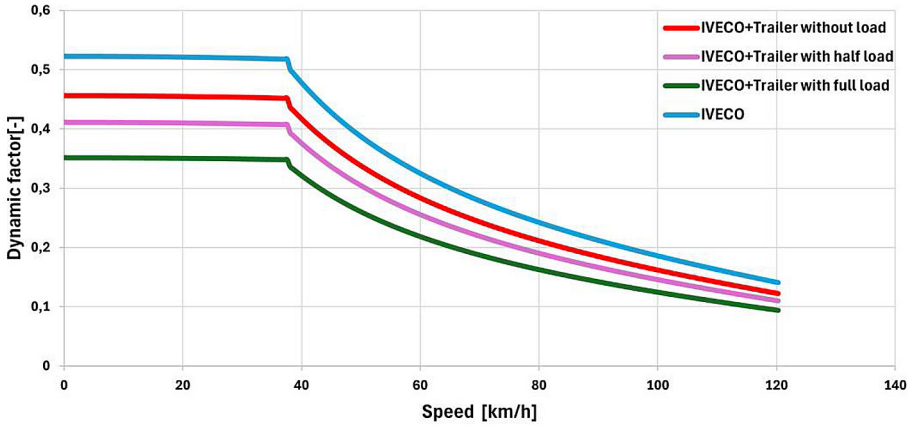

Figure 11. Dynamic indicator curves for different variants

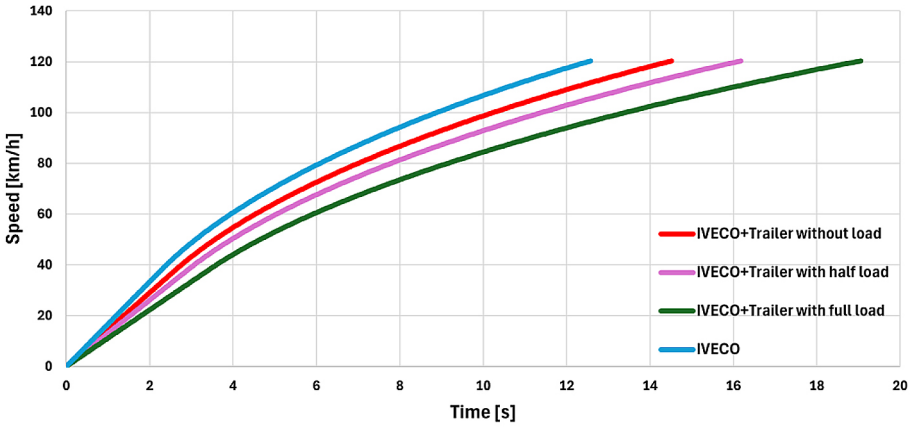

Figure 12. Acceleration characteristics

speed for the WLTC profile is 46.5 km/h. Figure 13b shows the speed changes in the cycle recorded by the author on the Bielsko-Biała (Poland) – Liptovský Mikuláš (Slovakia) section, designated BB-LM. The average speed of the cycle was 61.4 km/h.

Figure 14a shows the second real cycle on the Tarnów (Poland) – Warszawa (Poland) section, designated T-W. This route is characterized by a long motorway section (from 7000 s to 12000 s of the cycle). Due to the high speeds, the average speed was 82.1 km/h. Figure 14b shows the last driving profile recorded by the author on the Ivachnová (Slovakia) – Tarnów (Poland) section, designated I-T. The average speed for this driving style was 65.9 km/h.

The braking force value F_h and the regenerative braking force value F_{hr} were determined using the relationship [29, 34]:

$$F_h = -F_{pp} + F_{bp} - F_{tp} \tag{9}$$

$$F_{hr} = F_h \cdot \alpha \tag{10}$$

where: F_h – braking force [N]; F_{hr} – regenerative braking force [N]; α – regenerative braking coefficient [-].

The braking force using friction brakes F_{hc} was determined from the relationship:

$$F_{hc} = F_h - F_{hr} \tag{11}$$

Figure 15 shows the module responsible for calculating the value of electrical energy recovered during the trailer braking process.

According to the physical relationships, the energy was calculated as the integral of the engine power over time and has the form of time [24–27]:

$$E_{sil} = \int_{t1}^{t2} P_{sil}(t)dt \tag{12}$$

where: E_{sil} – recovered energy [J]; $P_{sil}(t)$ – instantaneous power [W].

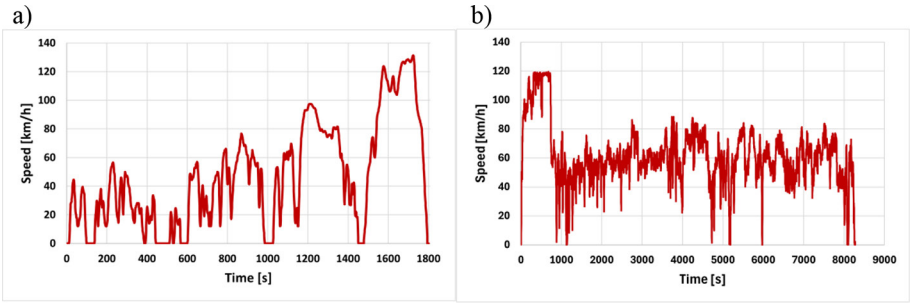

Figure 13. Speed curve: (a) for the WLTC cycle [23], (b) for the BB-LM cycle

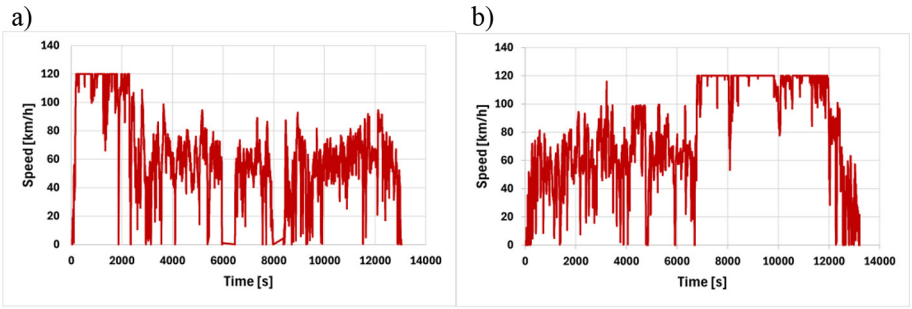

Figure 14. Speed curve: (a) for the T-W cycle, (b) for the I-T cycle

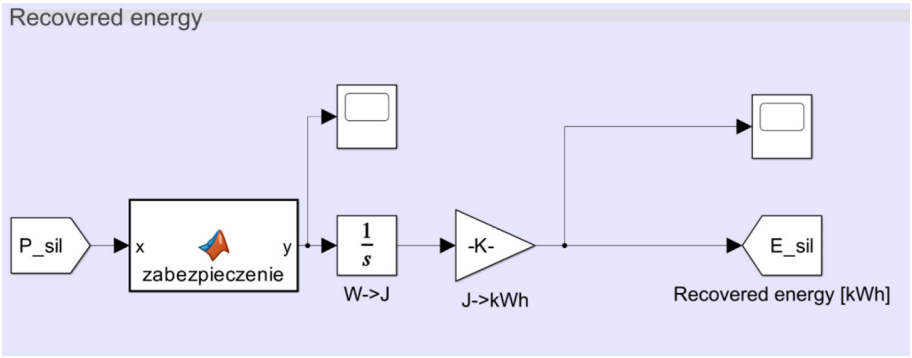

Figure 15. Block for calculating the energy recovered by the trailer system

The "protection" block contains code to prevent the creation of infinite or undefined values (e.g., division by zero). If the program detects such a value, it inserts a zero. The code is shown in Figure 16. After performing calculations according to formula (11), it converts the value to kilowatt-hours.

Figure 17 shows the subsystem responsible for calculating the percentage share of a given braking type – regenerative braking or braking using friction brakes.

The calculation method was based on the energy approach, taking into account the force of a given braking type as well as the vehicle speed. The total braking force was calculated using formula (8), the regenerative braking force using formula (9), and the braking force of friction brakes using formula (10). The energy dissipated by regenerative braking was determined using formula [26–28]:

$$E_{rek} = \int_{t1}^{t2} F_{hr}(t) \cdot v(t) \cdot dt \qquad (13)$$

where: E_{rek} – energy dissipated by regenerative braking [J]; $F_{hr}(t)$ – instantaneous regenerative braking force [N]; $v(t)$ – instantaneous trailer speed [m/s].

The energy dissipated by the friction brakes was calculated using the relationship [26–28]:

```
function y = zabezpieczenie(x)

if isnan(x) || isinf(x)
    y = 0;
else
    y = x;
end
end
```

Figure 16. Code from the "security" block

$$E_{cier} = \int_{t1}^{t2} F_{hc}(t) \cdot v(t) \cdot dt \tag{14}$$

where: E_{cier} – energy dissipated by friction brakes [J]; $F_{hc}(t)$ – instantaneous braking force of friction brakes [N].

The total energy is equal to the sum of both calculated energies. The percentage of each type of energy is determined [37–39]:

$$\eta_{rek} = \frac{E_{rek}}{E_{cał}} \cdot 100\% \tag{15}$$

$$\eta_{cier} = \frac{E_{cier}}{E_{cał}} \cdot 100\% \tag{16}$$

where: η_{rek} – regenerative braking efficiency [%]; η_{cier} – friction braking efficiency [%].

Figure 18 shows the energy efficiency calculation block. It calculates the energy efficiency of the trailer's energy recovery system.

The calculations are based on the relationship [26–29]:

$$\varepsilon = \frac{E_{sil}}{E_{cał}} \cdot 100\% \tag{17}$$

where: ε – energy efficiency [%].

Figure 19 shows a graph illustrating the amount of energy recovered during regenerative braking in four different driving cycles. For each driving condition, three trailer load variants were tested: empty, half-loaded, and fully loaded.

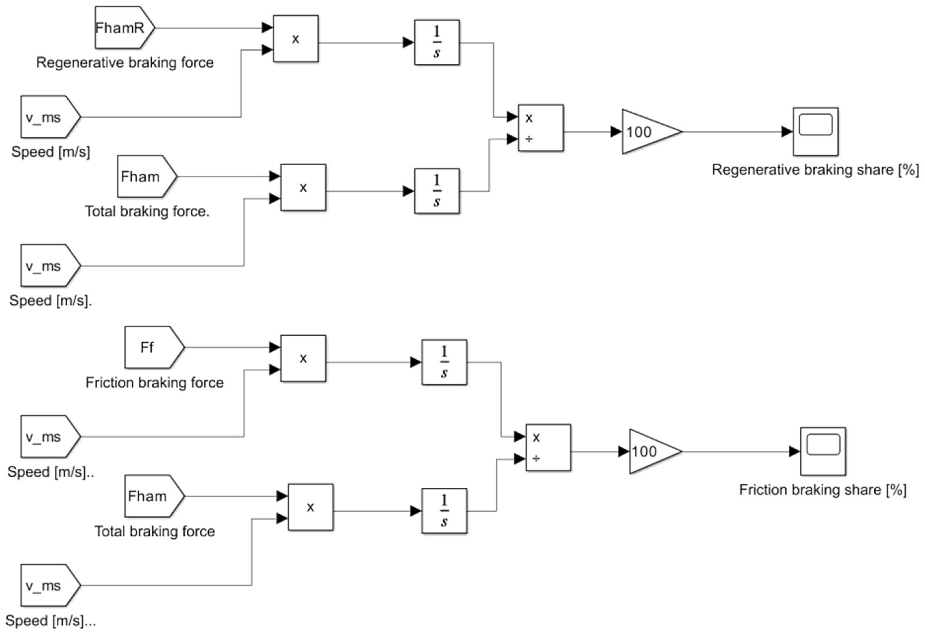

Figure 17. Block calculating the share of trailer braking types

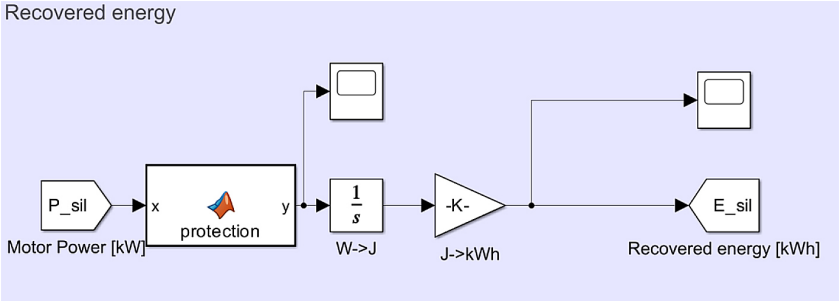

Figure 18. Energy efficiency calculation block

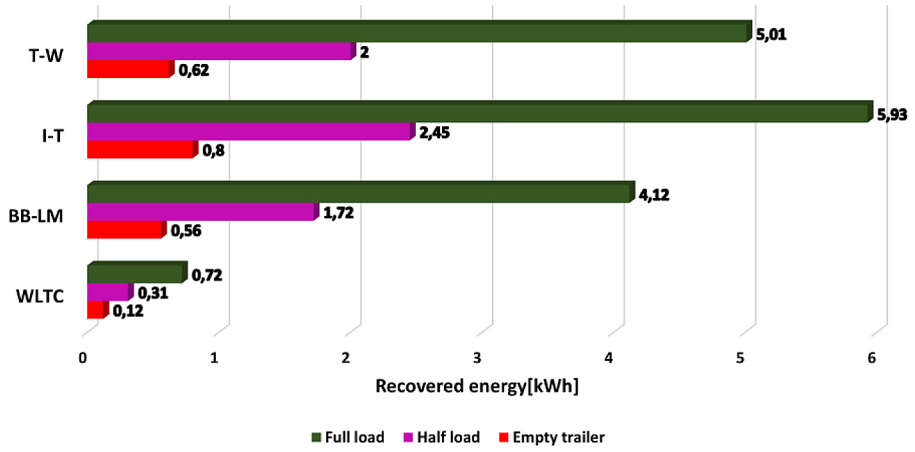

Figure 19. Amount of recovered energy by the modified car trailer

The simulation results confirm a strong relationship between trailer weight and the amount of recovered energy. For the route with the highest recovery (Ivachnová – Tarnów), we can observe the following percentage increase compared to an empty trailer: the amount of recovered energy is over 200% higher at half load, and over 600% higher at full load. This is due to the kinetic energy relationship. [30]:

$$E_{kin} = \frac{1}{2} \cdot m \cdot v^2 \tag{18}$$

The difference in the amount of recovered energy results from several factors: distance travelled, number of braking cycles, braking intensity, different initial speeds before braking, terrain, and road traffic congestion. Increasing mass while maintaining constant speed proportionally increases the kinetic energy of the moving vehicle. The average energy recovery for each cycle is presented in the Table 2.

Figures 20–23 present the energy recovery curve for each assumed driving profile with a fully loaded trailer. Despite the route between Bielsko-Biała-Liptovský Mikuláš and Tarnów-Warsaw being almost twice as short, the difference in recovered energy is small, especially for the empty trailer variant and the one with half the load. This is likely due to the characteristics of the recorded roads. The BB-LM section includes mainly roads in mountainous terrain and in cities, which translates into frequent braking. Another aspect negatively affecting energy recovery for the Tarnów-Warsaw section is the motorway section.

Table 2. Average amount of energy recovered during regenerative braking

Driving profile	Average amount of recovered energy [kWh]
WLTC	0.38
BB-LM	2.13
I-T	3.06
T-W	2.54

Long-term driving at a constant speed results in few or no braking cycles. Therefore, the trailer's energy recovery system is either unused or used only sparingly. Figure 24 shows a graph of the percentage of braking used by a given type (regenerative braking or friction braking) in the assumed driving cycles under three different trailer loads.

The results obtained in the graph above show a similar relationship to that observed for recovered energy with the moving trailer's mass. As the mass increases, the share of regenerative braking in the trailer's braking process increases. In the standardized WLTP cycle, a 6.92 percentage point increase can be observed between an empty and a fully loaded trailer. Similar relationships are observed for each driving profile tested. These values are presented in Table 3. Higher mass increases kinetic energy at the same trailer speed. When the system recovered more energy, the share of regenerative braking also increased. A significant difference in the share of the energy recovery system is visible between the standardized cycle and the actual driving profiles.

The average share of regenerative braking in the WLTC case was 57.47%, and for the Ivachnová-Tarnów (I-T) route it was 72.11%. This difference amounts to 14.64 percentage points. The high disproportion between the standardized and the actual cycle results from: the number of braking cycles, braking intensity, and the

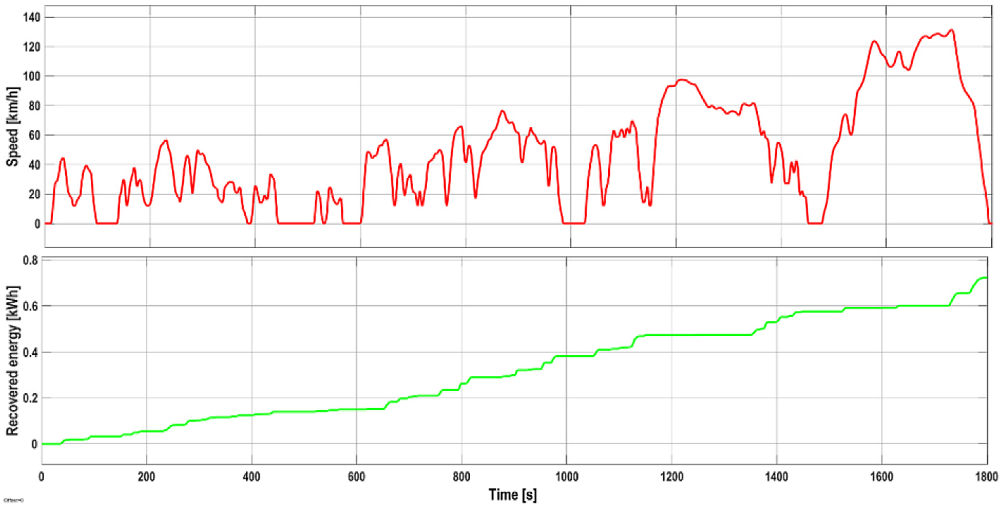

Figure 20. The amount of recovered energy depending on vehicle speed for the WLTC cycle with a full trailer load

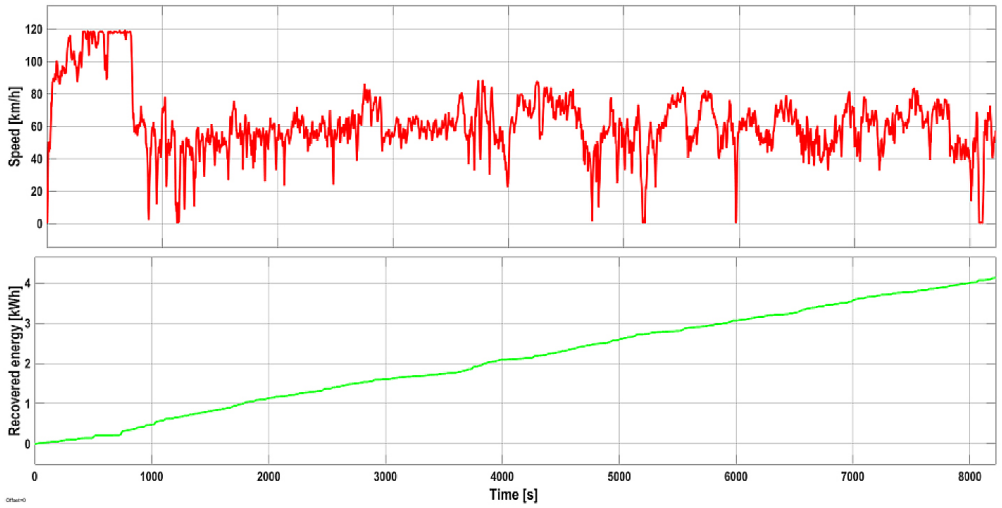

Figure 21. The amount of recovered energy depending on the vehicle speed for the Bielsko-Biała – Liptovský Mikuláš cycle with a fully loaded trailer

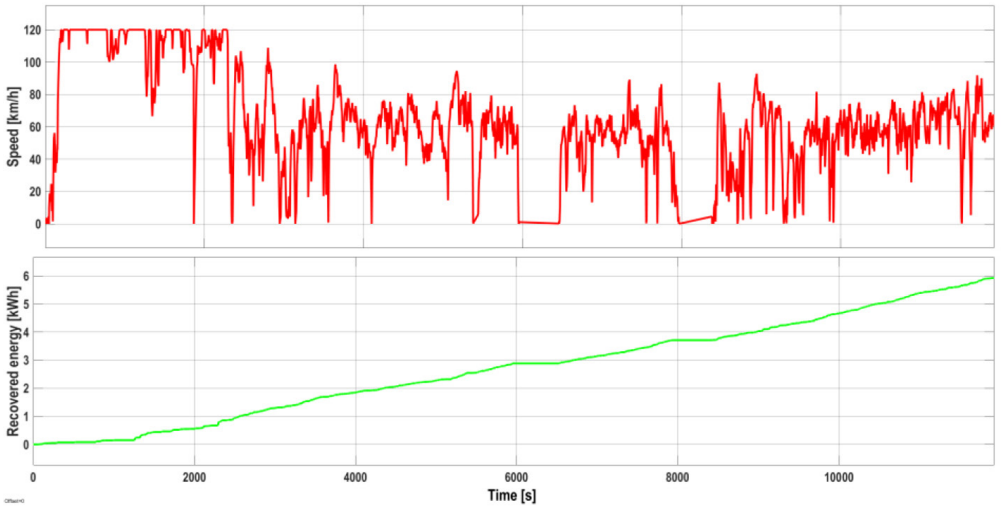

Figure 22. Graph showing the amount of recovered energy depending on the vehicle speed for the Ivachnová-Tarnów cycle with a fully loaded trailer

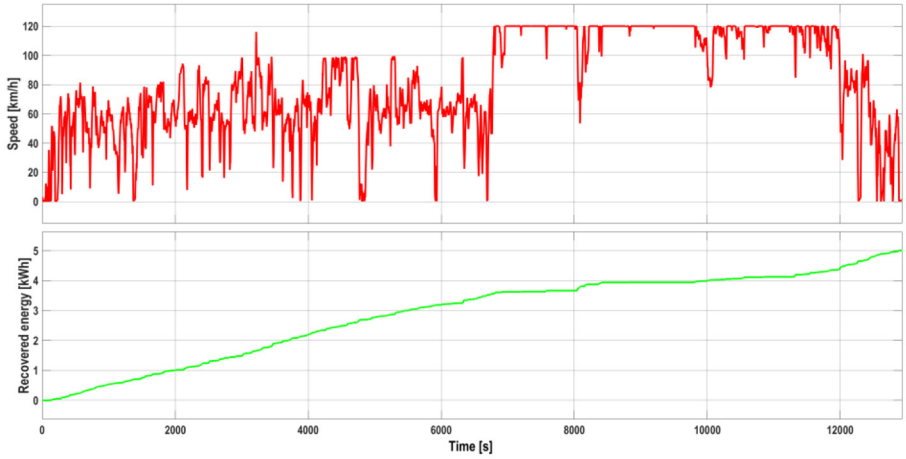

Figure 23. The amount of recovered energy depending on vehicle speed for the Tarnów – Warsaw cycle with a fully loaded trailer

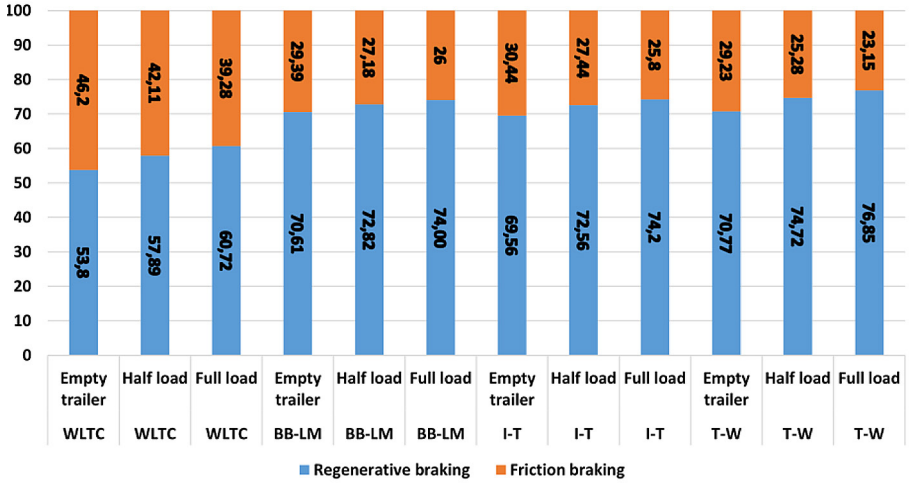

Figure 24. The contribution of a given braking type for all assumed driving cycles

Table 3. The effect of mass on the proportion of regenerative braking

Driving profile	Percentage increase over empty trailer for half load	Percentage increase from empty trailer to full load
WLTC	4.09	6.92
BB-LM	2.21	3.39
I-T	3	4.64
T-W	3.95	6.08

speed at which the braking process begins. Some of the actual cycles were recorded in mountainous areas, which translates into frequent speed reductions. All driving profiles recorded by the author reflect real road conditions, they represent driving on urban sections and expressways. The share and efficiency of the recuperative system increases with increasing vehicle speed [31–34], which results from the increasing value of kinetic energy. Table 4 presents characteristic parameters: duration, distance, and average speed during the trips. The highest average speed was achieved on the T-W route, at 82.1 km/h. This section also had the longest duration and the greatest distance traveled. The high average speed on this section results from the significant

Table 4. Characteristic parameter values during runs

Driving profile	Duration [s]	Distance [km]	Average speed [km/h]
WLTC	1 800	23.25	46.5
BB-LM	8 824	147	61.4
I-T	11 929	239	65.9
T-W	12 933	300	82.1

share of the motorway section in the cycle under consideration. The standardized WLTC cycle has the shortest duration among the variants tested. The significant participation of the electric machine in the braking process generates advantages: reduced wear of the conventional braking system, reduced operating costs, reduced brake dust emissions, reduced wear of the overrun system, and an impact on the braking dynamics of the vehicle and trailer combination. A greater share of recuperation reduces wear of brake pads and discs, a phenomenon observed in hybrid and electric vehicles [35, 36]. Using the proposed system controlled by CAN bus signals, it leads to a reduction in the response delay of the overrun brake. This will have a positive impact on the dynamics of the vehicle + trailer assembly; the delay caused by the trailer "running over" the vehicle's ball coupling during braking will be reduced by the energy recovery system initiating braking. Earlier initiation of the trailer braking process can also positively impact lower wear on the overrun system. In emergency situations, for example, when the brakes or overrun system are worn, the energy recovery system will assist the vehicle + trailer assembly in braking. An excessively worn trailer braking system can extend braking distances by up to 40% [33, 34]. Another benefit associated with the significant use of the regenerative brake is the reduction of brake dust. According to research, the use of energy recovery in hybrid and electric vehicles reduces brake dust emissions by 60% [35, 36]. Figure 25 presents the energy efficiency values – relationship (16).

For each of the four driving profiles, three series of tests were conducted with varying trailer loads. Energy efficiency increases with increasing load, but the difference between a half-loaded trailer and a full load is insignificant. The lowest values were achieved for an empty trailer; this relationship also results from the change in available kinetic energy; reducing mass causes a decrease in energy. Average energy efficiency values are presented in Table 5.

For each of the assumed driving conditions, the average energy efficiency values are similar. The highest efficiency level was achieved for the standardized WLTC cycle, with an average value of 72.17%, and for a full trailer load, 78.36%. This is due to fewer braking cycles than in actual driving cycles. The slightly lower efficiency for the recorded cycles may also result from the irregular number and duration of braking. The obtained high energy efficiency results most likely result from the assumed recuperation share

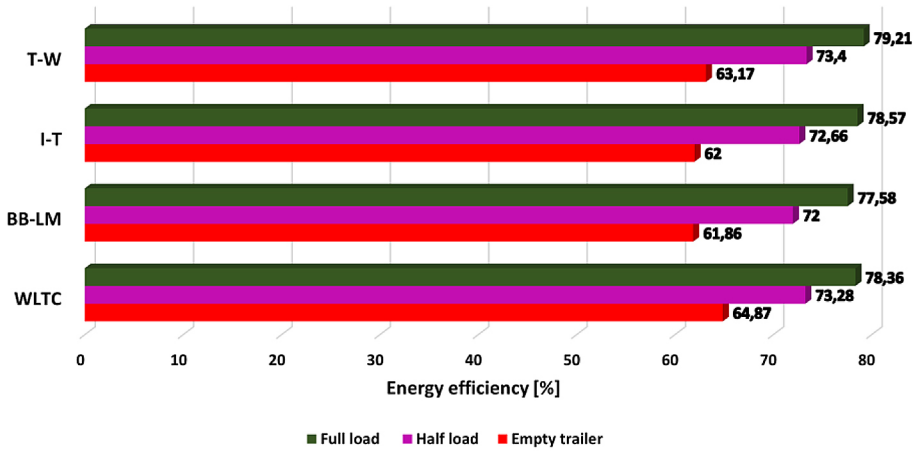

Figure 25. The energy efficiency of the regenerative braking process for each driving profile

Table 5. Average energy efficiency values for the adopted driving cycles

Driving profile	Average energy efficiency value [%]
WLTC	72.17
BB-LM	70.48
I-T	71.08
T-W	71.93

index in the process of 50 braking cycles. These are reflected in reality; according to available research, similar values were achieved for modern electric and hybrid vehicles [24, 31]. High efficiency, along with increasing trailer weight, suggests using the trailer's full load capacity as often as possible before completing a journey. At the same time, the impact of the vertical load exerted by the trailer on the coupling device on the towing vehicle's steering and stability should be taken into account [36].

CONCLUSIONS

This work addresses the concept of electric energy recovery in a trailer. Traction calculations were performed for an IVECO eDaily vehicle in several variants: with an empty trailer, with a half-loaded trailer, and with a fully loaded trailer. Motion resistance was determined, and characteristics were constructed: power balance, dynamic index, and vehicle acceleration for each trailer load condition.

The authors presented a proposal for energy recovery during trailer braking. Generally speaking, the process of energy recovery in cars is not new; it is already commonplace. However, energy recovery in vehicles such as trailers and semi-trailers is something new, and is only just being explored worldwide. The authors proposed an example of a specific solution. This is the authors' original contribution.

Four driving profiles were selected for simulation studies: one standardized WLTC cycle and three actual cycles. Three series of simulation tests were conducted, taking into account three trailer load variants: no load, half load, and full load. Based on the simulation results, graphs were developed: the amount of recovered energy, the percentage share of the given braking system, and the efficiency of regenerative braking. The highest value of recovered energy was obtained for the simulation on the Ivachnová-Tarnów section; at full load, 5.9 kWh of electricity was recovered. Calculations indicate economic benefits. For a 1.6 kW refrigeration unit, the amount of recovered energy allows for 3.5 hours of maximum power. A high share of regenerative braking generates benefits: reduced wear of the conventional braking system, reduced operating costs, reduced brake dust emissions, reduced wear of the overrun system, and an impact on the braking dynamics of the vehicle and trailer combination. Using CAN bus control will cause the regenerative braking system to react when the foot is lifted off the accelerator. This will improve driving dynamics, as the trailer will begin braking immediately, rather than when the overrun system is activated. The electric motor in the proposed system is engaged via the clutch only during deceleration. It is not used for propulsion, so it does not consume energy to move the vehicle combination.

The proposed energy recovery system is justified: economically, environmentally, and can improve user comfort. Traction calculations showed a significant impact of the weight attached to the trailer's towing vehicle on driving dynamics. Simulation studies demonstrated a significant contribution of regenerative braking to the braking process. The maximum amount of recovered energy allowed for cooling the trailer body at maximum power for 3.5 hours. Using a trailer with a braking energy recovery system by transport companies, particularly in the food sector, can bring significant economic benefits, resulting in a rapid return on investment. Less frequent replacement of braking system components, in addition to reducing costs, also contributes to reducing waste generation. One of the advantages of the proposed system is its wide range of applications. Caravan users can implement a similar system, allowing them to charge the on-board battery powering the trailer's utility equipment without the need for a power connection.

The implementation of regenerative braking support in an O2 category trailer is justified both technically and economically. The simulation results demonstrated a recovery potential of up to 5.4 kWh, which can be effectively utilized to power onboard systems such as a refrigeration unit. The effectiveness of the system increases with trailer mass and braking intensity, making it particularly beneficial for urban and distribution transport applications.

REFERENCES

1. The European Automobile Manufacturers' Association (ACEA). (2025, september). New car registrations: -0.1% in August 2025 year to date; battery-electric 15.8% market share. European Automobile Manufacturers' Association. https://www.acea.auto/pc-registrations/new-car-registrations-0-1-in-august-2025-year-to-date-battery-electric-15-8-market-share/ (access 2025.02.20)
2. Król, E., Hamowanie odzyskowe jako efektywny sposób zwiększenia zasięgu pojazdu hybrydowego. Napędy i Sterowanie, 2014;16(11): 116–119
3. KineticTraction Systems, (2015) Flywheel energy storage rail aplications https://kinetictraction.com/wpcontent/uploads/2015/07/KTSi.Brochure_FLYWHEEL.RAIL_.pdf (access 2025.02.20)
4. Jackiewicz, J. A flywheel based regenerative braking system for railway vehicles. Acta Mechanica et Automatica, 2023; 17: 52–59. https://doi.org/10.2478/ama 2023 0006
5. Urbaniak, M., Jacyna, M., Kardas-Cinal, E. Metody wykorzystania energii z rekuperacji w transporcie szynowym. Technika Transportu Szynowego. 2016; 12: 355–359.
6. Juda, Z. Hamowanie odzyskowe pojazdów z napędem elektrycznym – strategie sprawności odzysku i komfortu jazdy. Politechnika Krakowska. 2014.
7. Guo, J., Wang J. and Cao, B. Regenerative braking strategy for electric vehicles, 2009 IEEE Intelligent Vehicles Symposium, Xi'an, China, 2009; 864–868. https://doi.org/10.1109/IVS.2009.5164393
8. Oleksowicz, S., Burnham, K., Gajek, A., On the legal, safety and control aspects of regenerative braking in hybrid/electric vehicles. Czasopismo Techniczne. Mechanika, R. 2012; 109(3-M): 139–155.
9. Thermo King Europe. (b.d) Axlepower by the road. Pobrano 17 listopada 2025. https://europe.thermoking.com/advancer/axlepower-powered-by-the-road
10. Zeller, T., Prişca, T., Cujic, P., Bank, D., Doppelbauer, M. System analysis of a braking energy recovery axle of truck trailer. International Conference on Electrical Machines (ICEM), Torino, Italy, 2024; 1–7. https://doi.org/10.1109/ICEM60801.2024.10700329
11. Present, S., Rexeis, M. Potential assessment of electrified heavy-duty trailers based on the methods developed for EU legislation (VECTO Trailer). Future Transportation, 2025; 5: 77. https://doi.org/10.3390/futuretransp5030077
12. Chen, R., Duan, Y. Research on energy recovery strategy in braking of electric tractor-semitrailer. *SAE Technical Paper*, 2025-01-8290. 2025. https://doi.org/10.4271/2025-01-8290
13. Li, S., Yu, B., Feng, X. Research on braking energy recovery strategy of electric vehicle based on ECE regulation and I curve. *Science Progress*, 2020; 103(1). https://doi.org/10.1177/0036850419877762
14. Pusty, T., Mieteń, M., Kupicz, W. Detection of the vehicle mass using dynamic response to sinusoidal steering excitation. *Bulletin of the Polish Academy of Sciences: Technical Sciences*. 2026. https://doi.org/10.24425/bpasts.2026.158299
15. Prochowski, L., Pusty, T., Gidlewski, M., Jemioł, L. Experimental studies of the car-trailer system when passing by a suddenly appearing obstacle in the aspect of active safety of autonomous vehicles. *IOP Conference Series: Materials Science and Engineering*, 2018; 421: 032024. https://doi.org/10.1088/1757-899X/421/3/032024
16. Prochowski, L., Ziubiński, M., Szwajkowski, P., Gidlewski, M., Pusty, T., Stańczyk, T. L. Impact of control system model parameters on the obstacle avoidance by an autonomous car-trailer unit: Research results. *Energies*, 2021; 14: 2958. https://doi.org/10.3390/en14102958
17. Pusty, T., Więckowski, D., Dębowski, A., Wesołowski, M., Barta, D. Experimental study of the effect of tire pressure and cab height of a tractor-trailer driver on driving comfort. *Transport and Telecommunication*, 2025; 26(2): 175–184. https://doi.org/10.2478/ttj-2025-0014
18. Wu, J., Zhang, N., Tan, D., Chang, J., Shi, W. A robust online energy management strategy for fuel cell/battery hybrid electric vehicles. International Journal of Hydrogen Energy, 2020; 45(27): 14093–14107. https://doi.org/10.1016/j.ijhydene.2020.03.091
19. Ustawa z dnia 4 kwietnia 2024 w sprawie warunków technicznych pojazdów oraz zakresu ich niezbędnego wyposażenia, Dz. U. z 2024 r. poz. 502.
20. 2012 Hyundai Sonata 8.5kW 270V BISG - ALPHA Map Package. Version 2023-03. Ann Arbor, MI: US EPA, National Vehicle and Fuel Emissions Laboratory, National Center for Advanced Technology, 2023.
21. ISO 11446 Road vehicles — Connectors for the electrical connection of towing and towed vehicles
22. Peak-system. (b.d) PCAN-USB FD. Pobrano 17 listopada 2025. https://www.peak-system.com/PCAN-USB-FD.365.0.html?&L=1
23. J1939 SAE Enhanced DBC combines the power of.
24. ACEA Task Force HDEI/BCEI. (2024). FMS-Standard description (Version 05). https://www.fmsstandard.com/Truck/down_load/fms%20document_v_05_vers.07.07.2024.pdf (access 2025.02.02)
25. eDAILY introduction.pdf: IVECO S.p.A. (2024). eDAILY introduction [PDF]. Materiały techniczne producenta
26. eDaily_MY24.pdf: IVECO S.p.A. eDaily MY24 [PDF]. Dokumentacja produktowa
27. Ubysz, A., 2010. Engine torque for acceleration

of rotational mass in vehicles. Journal of KONES, 2024; 17(4): 553–560.

28. Arczyński, S. Mechanika ruchu samochodu. Warszawa: WNT. 1993.
29. Prochowski, L. Pojazdy samochodowe. Mechanika ruchu. Warszawa: WKiŁ. 2001.
30. Radzajewski, P., Guzek, M. Braking of the tractor-semi-trailer set in a rectilinear motion. WUT Journal of Transportation Engineering. 2021; 133: 39–58. https://doi.org/10.5604/01.3001.0015.6499
31. Kamiński, Z. Calculation of the optimal braking force distribution in three-axle trailers with tandem suspension. Acta Mechanica et Automatica. 2022; 16: 189–199. https://doi.org/10.2478/ama-2022-0023
32. Tutuianu M., Bonnel P., Ciuffo B., Haniu T., Ichikawa N., Marotta A., Pavlovic J., Steven H. Development of the world-wide harmonized light duty test cycle (WLTC) and a possible pathway for its introduction in the European legislation. Transportation Research Part D-Transport and Environment 2015; 40; 61–75. JRC97024.
33. Kropiwnicki, J., Gawłas, T. Estimation of the regenerative braking process efficiency in electric vehicles. Acta Mechanica et Automatica. 2023; 17: 303–310. https://doi.org/10.2478/ama-2023-0035. 57
34. Online Consortium of Oklahoma. Electric Power and Energy. 2020.https://open.ocolearnok.org/physicalscience/chapter/electric-power-and-energy/
35. Geng, C., Ning, D., Guo, L., Xue, Q., Mei, S. Simulation research on regenerative braking control strategy of hybrid electric vehicle. Energies. 2021; 14: 2202. https://doi.org/10.3390/en14082202
36. Yin, Z., Ma, X., Su, R., Huang, Z., Zhang, C. regenerative braking of electric vehicles based on fuzzy control strategy. Processes. 2023; 11: 2985. https://doi.org/10.3390/pr11102985
37. Gajek, A., Strzępek, P., Examining the braking energy recovery in a vehicle with a hybrid drive system. Archiwum Motoryzacji, [online] 2015; 68(2): 49–60, 159–170. http://yadda.icm.edu.pl/baztech/element/bwmeta1.element.baztech-8d3e7e88-7658-4ac7-b09f-e64c2f95ccd5
38. Zhu, Y., Wu, H., Zhang, J. Regenerative braking control strategy for electric vehicles based on optimization of switched reluctance generator drive system. IEEE Access. 2020; 1–1. https://doi.org/10.1109/ACCESS.2020.2990349
39. The RV Geeks. (b.d.). Trailer brake system. https://www.thervgeeks.com/trailer-brake-system/ (access 2025.10.23)
40. Robitschek, D., Kopacek, P., From mechanical to regenerative braking - Implications of the transition towards electric mobility on aspects of deceleration and tribological brake additives. 2021. https://doi.org/10.34726/hss.2021.81433
41. Hicks, W., Green, D. C., Beevers, S. Quantifying the change of brake wear particulate matter emissions through powertrain electrification in passenger vehicles, Environmental Pollution, Volume 2023; 336: 122400, https://doi.org/10.1016/j.envpol.2023.122400
42. Kąkol, M., Kuśmierz, D., Lozia, Z., Wpływ niehamowanej przyczepy jednoosiowej na długość drogi zatrzymania samochodu dwuosiowego. Paragraf na Drodze, 2023; 1: 55–73.
43. Luty, W., Simulation-based analysis of the impact of vehicle mass on stopping distance. Eksploatacja i Niezawodność, 2018; 20(2): 182–189.
44. Järvinen, A., Hoivala, J., Saarikoski, S., Aurela, M., Harni, S. D., Kylämäki, K., Rönkkö, T., Aakko-Saksa, P. Effect of pad material and regenerative braking on brake wear emissions. S9-2. Abstract from 28th ETH Nanoparticle Conference, Zürich, Switzerland. 2025.
45. Więckowski D., Pusty T., Jędrys P., Influence of the vertical load exerted by the trailer on the coupling device on towing vehicle's steerability and stability. IOP Conference Series: Materials Science and Engineering, Volume 148, Scientific Conference on Automotive Vehicles and Combustion Engines (KONMOT 2016) 22–23 September 2016, Krakow, Poland.